Letters on Materials 10 (1), 2020 pp. 78-82 www.lettersonmaterials.com

https://doi.org/10.22226/2410-3535-2020-1-78-82 PACS: 81.30.Kf

Superelasticity and its cyclic stability in [001]-oriented single crystals and oligocrystals of FeMnAlNi alloy in compression

V. V. Poklonov†, I. V. Kuksgauzen, Yu. I. Chumlyakov, D. A. Kuksgauzen, V. A. Kirillov

†poklonov_vyacheslav@mail.ru

Siberian Physical-Technical Institute of the National Research Tomsk State University,
1 Novosobornaya Sq., Tomsk, 634050, Russia

Superelasticity and stability of superelasticity in isothermal loading/unloading cycles under compression up to 3.5 – 4% at room temperature were studied in [001]-oriented $Fe_{43.5}Mn_{34}Al_{15}Ni_{7.5}$ (at.%) single crystals and $Fe_{42.5}Mn_{34}Al_{15}Ni_{7.5}Ti_{1}$ (at.%) oligocrystals (polycrystals with a large grain size of ~1000 μm) at the α-γ′-martensitic transformation. Using dynamic mechanical analysis and *in situ* cooling/heating in a microscope column, it was found that after quenching from 1473 K with water and ageing at $T = 473$ K for 3 hours, cooling-induced martensite in these crystals was not observed. Stress-induced martensite developed during deformation under a compressive load, wherein the critical stresses necessary for the stress-induced α-γ′-martensitic transformation changed only slightly when the test temperature increased. The α values characterizing this growth were 0.56 and 0.33 MPa/K for the [001]-oriented single crystal and oligocrystal, respectively. Superelasticity in these crystals was observed in a wide temperature range from 203 to 473 K. The maximum superelasticity achieved at room temperature was 6.2% and 5% in single- and oligocrystals, respectively. Single crystals exhibited good stability in loading/unloading cycles, in contrast to oligocrystals. Almost complete degradation of the superelasticity loop was observed after 40 and 20 cycles in single and oligocrystals, respectively. Degradation of the functional properties under cyclic influences was associated with the appearance of residual martensite. In single crystals, large martensite lamellae were optically observed predominantly in one system. In oligocrystals, several martensite systems interact, which leads to greater energy dissipation and a faster degradation of functional properties compared to single crystals.

Keywords: single crystal, oligocrystal, martensitic transformation, superelasticity, cyclic stability.

УДК: 539.371, 548.55

Сверхэластичность и ее циклическая стабильность в [001]-монокристаллах и олигокристаллах сплава FeMnAlNi при деформации сжатием

Поклонов В. В.†, Куксгаузен И. В., Чумляков Ю. И., Куксгаузен Д. А., Кириллов В. А.

Сибирский физико-технический институт Национального исследовательского Томского государственного университета, пл. Новособорная, 1, Томск, 634050, Россия

На [001]-ориентированных монокристаллах $Fe_{43.5}Mn_{34}Al_{15}Ni_{7.5}$ (ат.%) и олигокристаллах (поликристаллы с крупным размером зерна более 1000 мкм) сплава $Fe_{42.5}Mn_{34}Al_{15}Ni_{7.5}Ti_{1}$ (ат.%) при развитии α-γ′-мартенситного превращения исследована сверхэластичность и стабильность сверхэластичности в изотермическом цикле нагрузка/разгрузка при деформации сжатием до 3.5 – 4% при комнатной температуре. Методами динамического механического анализа и *in-situ* охлаждения/нагрева в колонне микроскопа установлено, что после закалки от 1473 К в воду и старения при $T = 473$ К, 3 часа в исследуемых кристаллах не наблюдается мартенсита охлаждения. При деформации под сжимающей нагрузкой развивается мартенсит напряжения, при этом критические напряжения, необходимые для развития α-γ′-мартенситного превращения под нагрузкой, слабо изменяются с ростом температуры испытания. Величина α, характеризующая этот рост, равна 0.56 и 0.33 МПа/К для [001]-монокристалла и олигокристалла, соответственно. Показано, что сверхэластичность в исследуемых кристаллах наблюдается в широком температурном интервале от 203 до 473 К. Максимальные значения сверхэластичности, достигнутые при комнатной температуре, равны 6.2% и 5% в моно- и олигокристаллах, соответственно. Монокристаллы проявляют хорошую стабильность в циклах нагрузка/разгрузка в отличие от олигокристаллов. Почти полная деградация петли сверхэластичности наблюдается после 40 и 20 циклов в моно- и олигокристаллах, соответственно. Деградация функциональных свойств при циклических воздействиях связана с появлением остаточного мартенсита. В монокристаллах оптически наблюдаются крупные ламели мартенсита преимущественно в одной системе. В олигокристаллах имеет место несколько систем мартенсита, которые взаимодействуют друг с другом, что приводит к большему рассеянию энергии и быстрой деградации свойств по сравнению с монокристаллами.

Ключевые слова: монокристалл, олигокристалл, мартенситное превращение, сверхэластичность.

1. Introduction

For the practical use of functional alloys with the shape memory effect and superelasticity (SE) as dampers, actuators or sensors, it is necessary to create an inexpensive high-strength material, one of the important technological characteristics of which is high resistance to thermomechanical fatigue.

The FeMnAlNi alloy, developed in 2011, is a good candidate for successful practical application due to a number of advantages. Firstly, in this alloy, an unusual mechanism of thermoelastic martensitic transformation (MT) from the high-temperature α (body-centered cubic lattice (bcc)) of austenite to γ′ (face-centered cubic lattice (fcc)) martensite is observed [1,2]. Secondly, the stresses σ_{cr}, which are necessary for the onset of stress-induced MT, change little when the test temperature increases. This contributes to the SE in a wide temperature range from 77 to 513 K [4–6]. The wide SE window, along with the low costs for constituent elements make FeMnNiAl alloys especially attractive.

However, there is a significant problem in the study and further practical application of FeMnNiAl alloys, which relates to the rapid diffusion over short distances of Mn and Al, which stabilize the γ-phase during quenching of these alloys. The γ-phase particles lead to partial or complete suppression of SE in both single crystals and polycrystals [3,7–10]. The γ-phase has a greater negative effect on polycrystals, since it is mainly released at the grain boundary, which leads not only to the suppression of SE, but also to embrittlement of the material. M. Vollmer et al. [10] showed that adding of 1.5% Ti in polycrystals suppresses the release of γ-phase particles; therefore, rapid quenching of polycrystals is not required. The SE value in polycrystals aged at $T=473$ K for 3 hours with 1.5% Ti was ~2.5%.

At present, the maximum value of SE in the FeMnNiAl alloy, equal to 7.2%, has been obtained for [001]-oriented single crystals with β-phase particles 6–10 nm in size [5]. Nanosized β-phase particles contribute to the hardening of the high-temperature phase and the suppression of plastic flow, leading to the observation of a larger value of SE ε_{SE} than in free-particle crystals ($\varepsilon_{SE}=3.6\%$) [5]. The maximum value of reversible strain of ~5% in polycrystals was achieved for crystals with a large grain size exceeding the cross section of the sample, the so-called oligocrystals [7]. Here, the creation of polycrystals with a large grain size plays a key role in obtaining large reversible strains. Large-sized grains were achieved by the authors of [7] using complex cyclic heat treatment. It should be noted that, in relation to the single crystals and polycrystals of the FeMnNiAl alloy, there are no data on the study of reversible strains during cyclic tests, which is an important characteristic in the practical use of these materials.

In connection with the foregoing, in this work, the SE and its cyclic stability in [001]-oriented $Fe_{43.5}Mn_{34}Al_{15}Ni_{7.5}$ (at.%) single crystals and $Fe_{42.5}Mn_{34}Al_{15}Ni_{7.5}Ti_1$ (at.%) oligocrystals with a large grain size were studied in compression.

2. Materials and methods

Single crystals with a nominal composition of $Fe_{43.5}Mn_{34}Al_{15}Ni_{7.5}$ (at.%) were grown using the Bridgman method in a helium atmosphere. In contrast to the previous study [10], $Fe_{42.5}Mn_{34}Al_{15}Ni_{7.5}Ti_1$ (at.%) oligocrystals were doped with a smaller amount of titanium (1% Ti) to suppress the release of the γ-phase along grain boundaries. A new approach was used to obtain oligocrystals (polycrystals with a large grain size of ~1000 μm). After melting, there was an additional passage of the crystals through a temperature gradient. In these oligocrystals, with the addition of 1% Ti, the grains were elongated along the compression direction with an average grain size of 1500–2000 μm. From Fig. 1, it can be seen that the grain boundaries were very thin and there were no characteristic teeth (Fig. 1a), which occur along the grain boundaries in Ti-free crystals with γ-phase particles (Fig. 1b [3]).

Samples for compression with gauge dimensions of 4×4×8 mm were cut using an electro-spark discharge machine. For investigation, [001]-oriented single crystals were chosen, in which, firstly, the theoretical lattice strain ε_0 for α-γ′-MT under compression has a maximum value (ε_0=10.5%) [2]. Secondly, in [001]-oriented crystals, according to the geometric loading conditions, twinning of γ′-martensite does not occur under loading, and the lattice strain at α-γ′-MT corresponds to the transformation strain during the formation of the correspondent variant pair (CVP) of γ′-martensite ε_{CVP} ($\varepsilon_0=\varepsilon_{CVP}$). Such a CVP-structure of martensite ensures the invariance and high mobility of the habit plane during MT. Before testing, the samples were quenched at 1473 K in water and then held at $T=473$ K for 3 hours. After ageing at $T=473$ K for 3 hours, ordered coherent particles of the B2-phase (NiAl) 6–10 nm in size and a volume fraction of 34.3% were precipitated in the bcc-matrix [5].

Mechanical tests were conducted on an Instron 5969 universal testing machine at a strain rate of $4\cdot10^{-4}$ s^{-1} in the temperature range from 203 to 473 K. The cyclic stability of SE was investigated during isothermal loading/unloading cycles in compression up to $\varepsilon_{applied}=3.5-4\%$ at room

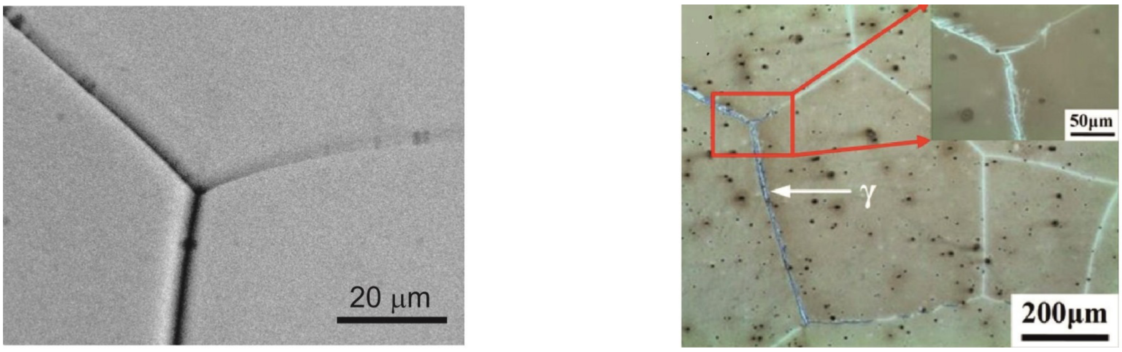

a b

Fig. 1. (Color online) Optical image of the studied $Fe_{42.5}Mn_{34}Al_{15}Ni_{7.5}Ti_1$ (at.%) oligocrystal (a) and $Fe_{42}Mn_{34}Al_{16.5}Ni_{7.5}$ (at.%) polycrystal without Ti-alloying after quenching from 1498 K [3] (b).

temperature ($T=298$ K). Dynamic mechanical analysis (DMA) DMA/SDTA861 (Mettler Toledo) and an *in situ* cooling/heating attachment (Linkam) were used to study α-γ′-MT during cooling/heating in the temperature range from 143 to 373 K. Metallographic investigations of the surface of the samples before and after the tests were performed using a Keyence VHX-2000 optical microscope and a TescanVega 3 scanning microscope. The *in situ* XRD were measured using a Dron-3 X-ray diffractometer.

3. Results and discussion

Investigations of the temperature dependence of the elastic modulus *E* by the DMA method showed that the modulus decreased almost linearly with increasing temperature and there was no pronounced softening of the elastic modulus, which would indicate a phase transformation in the measured temperature range. In addition, cooling-induced martensite was not detected during *in situ* cooling/heating in a microscope column. Only stress-induced martensite was observed in these alloys. Fig. 2 shows the critical stresses σ_{cr} necessary for the stress-induced α-γ′-MT in the temperature range from 203 to 523 K for [001]-oriented $Fe_{43.5}Mn_{34}Al_{15}Ni_{7.5}$ (at.%) single crystals (curve 1) and $Fe_{42.5}Mn_{34}Al_{15}Ni_{7.5}Ti_1$ (at.%) oligocrystals (curve 2). The stresses σ_{cr} slightly increased when the test temperature increased. The α values characterizing this growth were 0.56 and 0.33 MPa/K for the [001]-oriented single crystal and oligocrystal, respectively. These values are close to the α values obtained in previous studies [4 – 7].

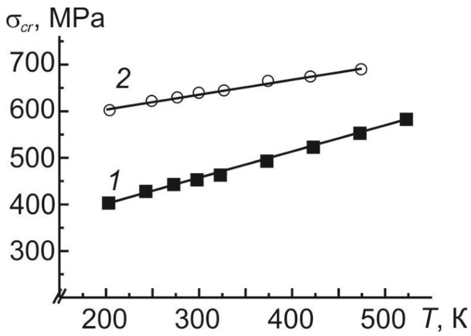

Fig. 2. Temperature dependence of critical stresses σ_{cr} necessary for the stress-induced α-γ′-MT for [001]-oriented $Fe_{43.5}Mn_{34}Al_{15}Ni_{7.5}$ (at.%) single crystals (curve 1) and $Fe_{42.5}Mn_{34}Al_{15}Ni_{7.5}Ti_1$ (at.%) oligocrystals (curve 2).

Superelasticity was observed in the entire studied temperature range both in single crystals and oligocrystals. Fig. 3 shows the stress-strain curves at $T=298$ K for [001]-oriented single crystals (Fig. 3a) and oligocrystals (Fig. 3b) in compression. It was established that the form of the σ(ε) curve and the maximum value of SE in the single crystals and oligocrystals differed. In single crystals at 3% applied strain at $T=298$ K, the stress σ_{cr} for the onset of the stress-induced MT was 450 MPa, and a perfect SE loop with a stress hysteresis Δσ of 150 MPa, characterizing energy dissipation, was observed. The stress-induced transformation proceeded with a strain hardening coefficient $\theta = d\sigma/d\varepsilon$ close to zero. When the applied strain increased from 3% to 8.5%, a decrease in stress σ_{cr} on 50 MPa, an increase in stress hysteresis up to 400 MPa and an accumulation of the irreversible strain up to 0.5% were observed. At a total applied strain of $\varepsilon_{applied}=7.5\%$, the SE reached a maximum value of 6.2%. With an increase in $\varepsilon_{applied}$, the SE value decreased and the value of irreversible strain increased. The SE value did not reach the theoretical resource for crystals of a given orientation, equal to 10.5%.

In oligocrystals with a total applied strain of 3.2%, the stress σ_{cr} was 640 MPa, the transformation proceeded with the coefficient θ other than zero, the wide stress hysteresis Δσ was 50 MPa, and an irreversible strain of 0.5% were observed. An increase in the applied strain to 5.7% led to a decrease in stress σ_{cr} to 500 MPa, an increase in stress hysteresis to 450 MPa and the accumulation of irreversible strain to 1.2%. In oligocrystals, the maximum value of SE at room temperature was 5%. This value is two times greater than the value obtained by the authors of [10] in polycrystals that were alloyed with 1.5% Ti.

It should be noted that a large stress hysteresis at α-γ′-MT and a large value of reversible strain at room temperature in single crystals ($\Delta\sigma=400$ MPa, $\varepsilon_{SE}=6.2\%$) and oligocrystals ($\Delta\sigma=450$ MPa, $\varepsilon_{SE}=5\%$) are important aspects in the design of industrial products, namely dampers.

Isothermal loading/unloading cycles under compression to $\varepsilon_{applied}=3.5-4\%$ at room temperature ($T=298$ K) were performed in order to study the cyclic stability of SE in single crystals and oligocrystals. Fig. 4 shows the curves obtained in this experiment and metallographic studies of residual martensite after 40 and 20 loading/unloading cycles for single crystals and oligocrystals, respectively. Fig. 4 shows that in the first loading/unloading cycle at $T=298$ K,

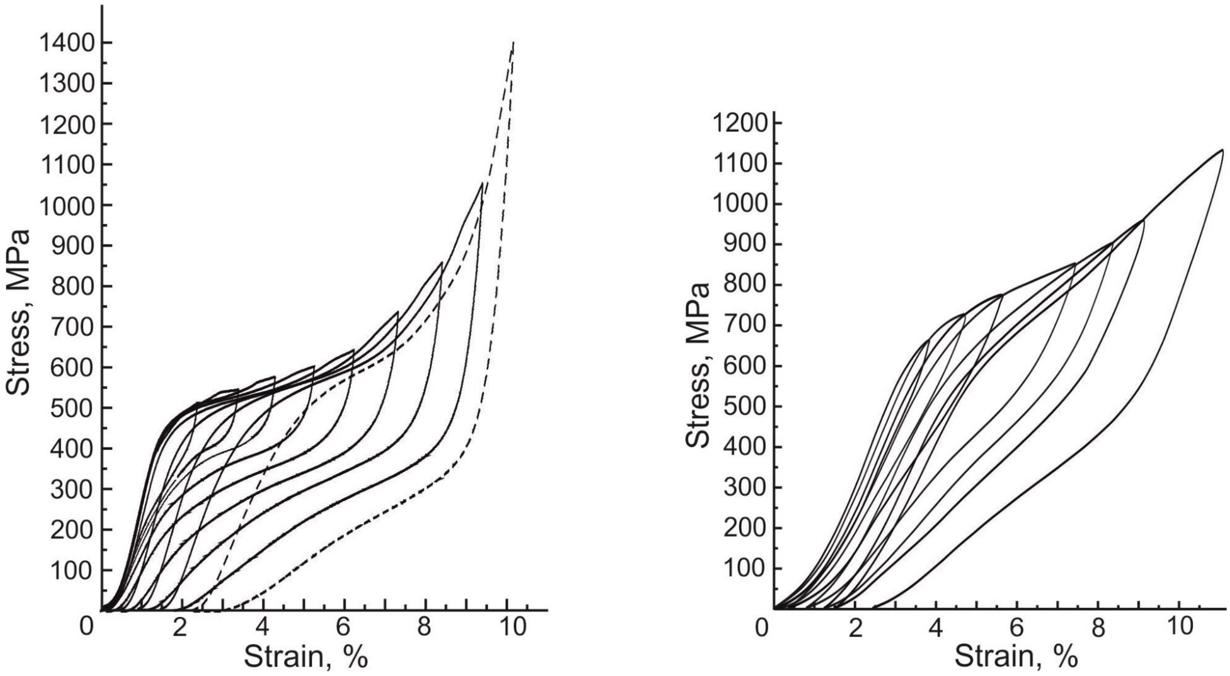

a b

Fig. 3. Stress-strain curves at $T = 298$ K for [001]-oriented $Fe_{43.5}Mn_{34}Al_{15}Ni_{7.5}$ (at.%) single crystals (a) and $Fe_{42.5}Mn_{34}Al_{15}Ni_{7.5}Ti_{1}$ (at.%) oligocrystals (b) in compression.

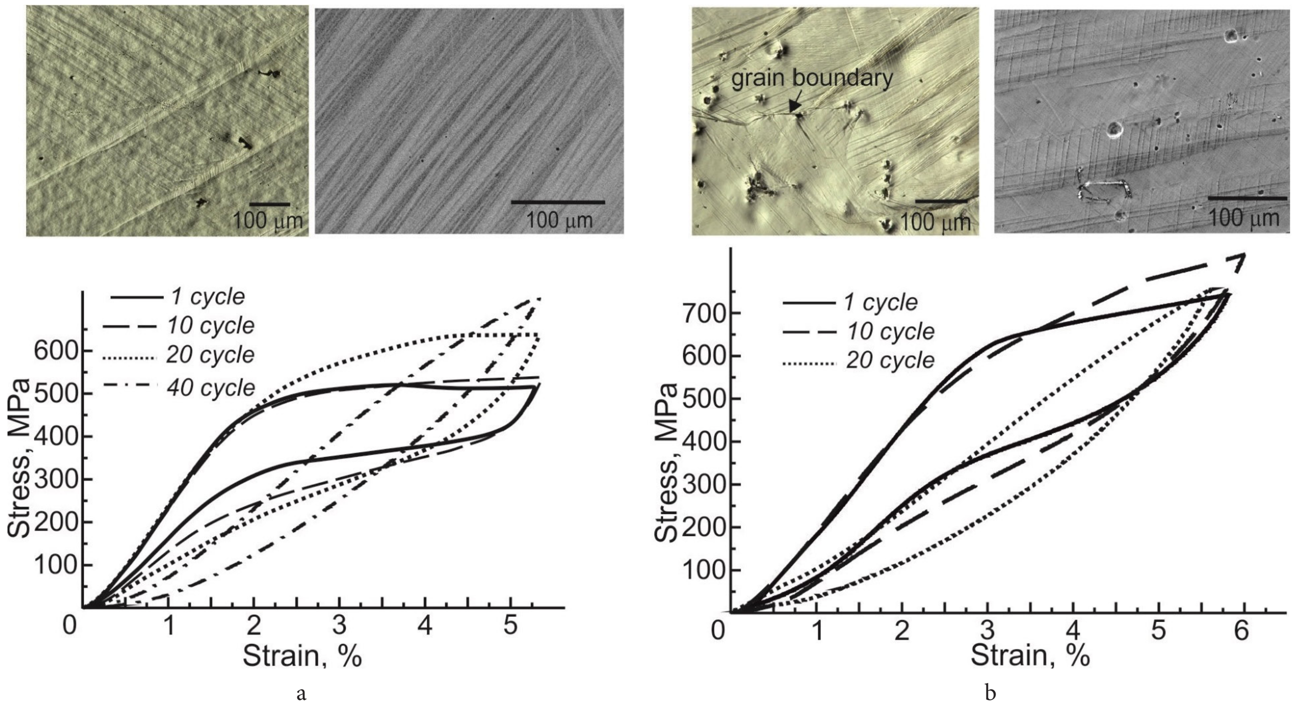

a b

Fig. 4. (Color online) The curves obtained in the loading/unloading cycle at $T = 298$ K and a metallographic image of the residual martensite on deformed samples in [001]-oriented $Fe_{43.5}Mn_{34}Al_{15}Ni_{7.5}$ (at.%) single crystals (a) and $Fe_{42.5}Mn_{34}Al_{15}Ni_{7.5}Ti_{1}$ (at.%) oligocrystals (b).

a perfect SE loop in single crystals and oligocrystals was observed. After 10 loading/unloading cycles in single crystals and oligocrystals, degradation of the SE was observed, which comprised a 1.3 – 1.5- fold increase in $\Delta\sigma$, reducing σ_{cr} stresses and changing the shape of the $\sigma(\varepsilon)$ curves. In oligocrystals, a residual strain of ~0.3% in the 10^{th} loading/unloading cycle was observed. When the number of cycles equaled 20, the effect of degradation increased. After 40 and 20 isothermal cycles in single crystals and oligocrystals, respectively, a complete change in the $\sigma(\varepsilon)$ curve was observed.

The degradation of functional properties during the loading/unloading cycle was associated with the appearance of residual martensite, which was detected optically on the surface of deformed samples (Fig. 4, insets). Results of *in situ* XRD patterns also show the stress-induced γ'-martensite on deformed samples. The sharp $(220)_{\alpha}$ peak from the initial bcc-structure and the $(222)_{\gamma'}$ peak from martensite with fcc structure are observed in the phase diagram (Fig. 5).

A greater accumulation of irreversible strain and a large fraction of residual martensite were observed in

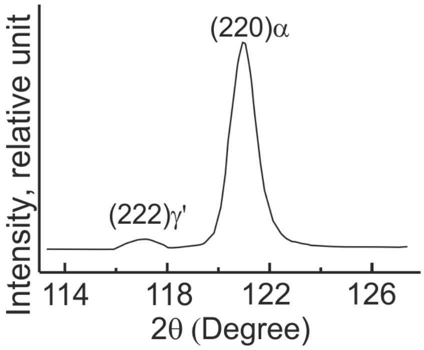

Fig. 5. *In situ* XRD patterns of [001]-oriented $Fe_{43.5}Mn_{34}Al_{15}Ni_{7.5}$ (at.%) single crystals after 40th isothermal cycle.

oligocrystals. In single crystals, large martensite lamellas were optically observed mainly in one system (Fig. 4a, inset). In oligocrystals, when stress-induced MT developed, several martensite variants nucleated in the field of one grain (Fig. 4b, inset). Martensite variants interacted with each other. As a result, a multivariant martensitic structure was formed, leading to greater energy dissipation and a faster degradation of functional properties compared to the single crystals.

The accumulation of residual martensite led to a high level of dissipated energy ΔG_{diss} during the transformation, which was characterized by the value of the stress hysteresis $\Delta\sigma$ and grew as the number of loading/unloading cycles increased. In [11], a criterion was proposed for predicting cyclic stability during the development of SE by analyzing the SE loop obtained in the first loading/unloading cycle. This criterion is as follows: it is necessary to achieve a state with a small value of energy dissipation ΔG_{diss} in comparison with the reversible energy stored during the stress-induced MT ΔG_{rev}, in order for the $\Delta G_{rev}/\Delta G_{diss}$ ratio to be greater than unity. The value of ΔG_{rev} can be estimated as the area under the unloading curve and ΔG_{diss} is the area inside the loading/unloading hysteresis loop. The estimated values of dissipation and irreversible energies in single crystals are 15.38 MJ/m^3 and 5.84 MJ/m^3, respectively, so that $\Delta G_{rev}/\Delta G_{diss}=2.63$. In oligocrystals ΔG_{rev}=18.73 MJ/m^3, ΔG_{diss}=9.58 MJ/m^3 and $\Delta G_{rev}/\Delta G_{diss}$=1.96. Therefore, in the first loop of the SE, it could be assumed that single crystals will exhibit greater cyclic stability, since the $\Delta G_{rev}/\Delta G_{diss}$ ratio in single crystals is 1.3-fold greater than in oligocrystals, which was experimentally found in this study.

4. Conclusions

1. On [001]-oriented $Fe_{43.5}Mn_{34}Al_{15}Ni_{7.5}$ (at.%) single crystals and $Fe_{42.5}Mn_{34}Al_{15}Ni_{7.5}Ti_1$ (at.%) oligocrystals after quenching at 1473 K in water and ageing at $T=473$ K for 3 hours, dynamic mechanical analysis and *in situ* cooling/heating in a microscope column showed that the α-γ′-martensitic transformation was not observed.

2. The studied crystals had a weak temperature dependence of the critical stresses necessary for the stress-induced α-γ′-martensitic transformation, with the α values were 0.56 and 0.33 MPa/K for the [001]-oriented single crystal and oligocrystal, respectively.

3. Single crystals and oligocrystals exhibited SE in a wide temperature range from 203 to 473 K. The maximum SE values achieved at room temperature were 6.2% and 5% in single crystals and oligocrystals, respectively.

4. Single crystals were characterized by lower energy dissipation and a larger $\Delta G_{rev}/\Delta G_{diss}$ ratio, which determines better resistance to cyclic loads at room temperature, compared with oligocrystals.

Acknowledgements. The reported research was funded by Russian Foundation for Basic Research and the government of the Tomsk region of the Russian Federation, grant № 19-43-703008.

References

1. P. Chowdhury, D. Canadinc, H. Sehitoglu. Mater. Sci. Eng., R. 122, 1 (2017). Crossref
2. A. Ojha, H. Sehitoglu. Int. J. Plast. 86, 93 (2016). Crossref
3. P. Huang, H. Peng, S. Wang, T. Zhou, Y. Wen. Mater. Charact. 118, 22 (2016). Crossref
4. L.W. Tseng, J. Ma, S.J. Wang, I. Karaman, M. Kaya, Z.P. Luo, Y.I. Chumlyakov. Acta Mater. 89, 374 (2015). Crossref
5. L.W. Tseng, J. Ma, B.C. Hornbuckle, I. Karaman, G.B. Thompson, Z.P. Luo, Y.I. Chumlyakov. Acta Mater. 97, 234 (2015). Crossref
6. L.W. Tseng, J. Ma, Y.I. Chumlyakov, I. Karaman. Scripta Mater. 166, 48 (2019). Crossref
7. T. Omori, H. Iwaizako, R. Kainuma. Mater. Des. 101, 263 (2016). Crossref
8. T. Omori, M. Okano, R. Kainuma. APL Materials. 1, 032103 (2013). Crossref
9. T. Omori, R. Kainuma. Shap. Mem. Superelasticity. 3, 322 (2017). Crossref
10. M. Vollmer, P. Krooß, I. Karaman, T. Niendorf. Scripta Mater. 126, 20 (2017). Crossref
11. N.G. Larchenkova. Zakonomernosti proyavleniya i tsyklicheskaya stabil'nost' funktsional'nyh svojstv geterofaznyh monokristallov splava NiFeGaCo s pamyat'yu formy. Dissertacija na soiskanie stepeni kandidata tehnicheskih nauk. Tomsk (2019) 185 p. (in Russian) [Н. Г. Ларченкова. Закономерности проявления и циклическая стабильность функциональных свойств гетерофазных монокристаллов сплава NiFeGaCo с памятью формы: дисс. канд. физ.-мат. наук. Томск (2019) 185 с.]